

A Numerical Solution Method for Two-dimensional Nonlinear Water Waves on a Plane Beach of Constant Slope

Young-Gill Lee¹, Jae-Kyung Heo², Kwang-Leol Jeong¹ and Kang-Sin Kim¹

¹ Dept. of Naval Architecture and Ocean Eng., Inha Univ., Incheon, KOREA;
E-mail: younglee@inha.ac.kr

² Ship Research Institute, Hanjin Heavy Industries Co., Ltd., Busan, KOREA

Abstract

Unsteady nonlinear wave motions on the free surface over a plane beach of constant slope are numerically simulated using a finite difference method in rectangular grid system. Two-dimensional Navier-Stokes equations and the continuity equation are used for the computations. Irregular leg lengths and stars are employed near the boundaries of body and free surface to satisfy the boundary conditions. Also, the free surface which consists of markers or segments is determined every time step with the satisfaction of kinematic and dynamic free surface conditions. Moreover, marker-density method is also adopted to allow plunging jets impinging on the free surface. The second-order Stokes wave theory is employed for the generation of waves on the inflow boundary. For the simulation of wave breaking phenomena, the computations are carried out with the plane beach of constant slope in surf zone. The results are compared with other existing experimental results. Agreement between the experimental data and the computation results is good.

Keywords: free surface, finite difference method, plane beach, nonlinear water waves, marker-density

1 Introduction

As waves approach the surf zone they begin to feel the sea bottom, become steeper and eventually break. The properties of breaking waves in surf zone provide coastal engineers with important clues to wave forces, coast erosion, sediment transport, etc. Numerous experiments were carried out to find the geometry and characteristics of the breaking waves. Recently, the procedure of plunging breaking is captured by flow visualization using a high-speed imaging system in a flume (Perlin and He 1996). And, Chen, et al. (1999) carried out numerical simulations describing plunging breakers including the splash-up phenomenon by using a two-dimensional Navier-Stokes simulation based on the VOF method. Galvin (1968) identified collapsing to describe an intermediate breaker type between plunging and surging. He also introduced an offshore parameter and an inshore parameter to classify the breaker types which are functions of wave steepness and a beach slope. These parameters were converted to ξ , the surf similarity parameter, by Battjes (1974). Smith and Kraus (1990) performed the laboratory experiments of breaking waves

on bar and trough beaches and showed that the transition values for the breaker type over the barred profiles are lower than those on plane slopes. Also, any research works on turbulent phenomena after breaking have been reported (Basco 1985, Battjes 1988, Hwung et al 1988). Hino et al. (1984) and Monaghan (1994) simulated the deformation of periodic waves on a beach by TUMMAC and SPH respectively. Koshizuka et al (1998) presented a numerical analysis method of breaking waves using the moving particle semi-implicit(MPS) method. Lin and Liu (1998) applied their numerical model for the treatment of breaking waves to the simulation of breaking waves in the surf zone.

In this paper, the accuracy of periodic waves numerically generated is tested with changing free surface movement techniques. In the numerical simulation of free surface waves, it is important to reduce numerical damping and diffusion and to have the waves flow through an outflow boundary with no influence inside computational domain. Various numerical techniques for the treatment of kinematic free surface condition are briefly introduced and compared to be used for the simulation of the breaking waves. The hybrid method is used for the simulation of plunging breakers and two-phase flow method(by using marker-density method) is adopted to simulate flow characteristics after waves break. The nine numerical tests of the breaking waves on beaches and the free surface simulations after waves break by two-phase flow method are carried out and the computational results are compared with some published experimental data.

2 Computational method

The governing equations for the present computations are the following Navier-Stokes equations and the continuity equation for two-dimensional incompressible viscous flows.

$$\frac{\partial u}{\partial t} + u \frac{\partial u}{\partial x} + w \frac{\partial u}{\partial z} = -\frac{1}{\rho} \frac{\partial p}{\partial x} + \frac{\mu}{\rho} \left(\frac{\partial^2 u}{\partial x^2} + \frac{\partial^2 u}{\partial z^2} \right) \quad (1)$$

$$\frac{\partial w}{\partial t} + u \frac{\partial w}{\partial x} + w \frac{\partial w}{\partial z} = -\frac{1}{\rho} \frac{\partial p}{\partial z} + \frac{\mu}{\rho} \left(\frac{\partial^2 w}{\partial x^2} + \frac{\partial^2 w}{\partial z^2} \right) + g \quad (2)$$

$$\frac{\partial u}{\partial x} + \frac{\partial w}{\partial z} = 0 \quad (3)$$

where u and w are the velocity components in the x and z directions, respectively. μ is the dynamic viscosity coefficient, ρ is the density, and g is the gravitational acceleration. For the computation of two-phase flow, the water and air regions are solved with the constant physical value of the density, respectively.

The governing equations are differentiated with a finite differencing scheme with a fixed staggered variable mesh system. The Adams-Bashforth scheme is adopted for the time integration of momentum equations. For the approximations of convection terms, a third order upstream scheme, a second order hybrid scheme and a first order upstream scheme are applied with the consideration of the number of neighboring fluid cells. The other spatial derivative terms are discretized by the centered differentiating scheme. Pressure distribution is obtained by the solution of the Poisson equation, and the SOR (Successive Over Relaxation) method is employed to solve the finite differencing form of this equation.

The No-slip condition is implemented with an irregular leg length for the calculation of differential terms around the body surface, and the flux calculation for divergence zero is

used in a body boundary cell which is involving the body surface. In each body boundary cell, the velocity and pressure are computed by a simultaneous iteration method until the pressure is converged.

The dynamic free surface boundary condition is satisfied in the present computation is $P = P_0$ on free surface. where P_0 is the atmospheric pressure. When the Poisson equation of pressure is solved near the free surface, irregular stars are employed to satisfy the dynamic free surface boundary condition.

The kinematic free surface boundary condition satisfied in the present computation is as follows:

$$\frac{D(z - \eta)}{Dt} = 0 \tag{4}$$

where η is the wave height. Eq.(4) shows that the normal velocities of the fluid particle on the free surface and the free surface boundary must be equal. One of the easy treatments of the Eq.(4) is to use marker particles moving with local velocity which is calculated from neighboring fluid cells. Heo and Lee (1996) compared the results of various methods associated with the kinematic free surface boundary condition and showed that the marker particle method is more accurate than the line-segment method. They combined the marker particle and line-segment methods to reduce numerical error and to simulate nonlinear free surface motion which is accompanied by breaking waves. However, the marker and line-segment methods are very difficult when addressing the nonlinear free surface motions after the breaking phenomena of waves. Therefore, the marker-density method is adopted in our computation for the satisfaction of the kinematic free surface boundary condition during the wave breaking process. The initial values are set equal to the physical values at the center of each cell. When each densities of gas and liquid are scalar value $\rho^{<1>}$ and $\rho^{<2>}$, M_ρ is defined as a scalar value of each density. The variation at the marker-density of each cell is defined by density function M_ρ . From the distribution of marker-densities the location of the interface between the two fluid regions is defined by an appropriate position in the intermediate region of the density function($\rho^{<1>}$ and $\rho^{<2>}$). That is, it is considered that the fluid of each cell in the intermediate region is mixed with two-phase fluids. However, it must be noticed that the marker-density is adopted only for the determination of the location of the interface. The physical value of density is used for solving the governing equations of fluid flow in each region, respectively.

The following is the transport equation of the density function, Eq. (5), is employed for the determination of the location of free surface instead of Eq. (4).

$$\frac{\partial M_\rho}{\partial t} + u \frac{\partial M_\rho}{\partial x} + w \frac{\partial M_\rho}{\partial z} = 0 \tag{5}$$

In order to satisfy the dynamic free surface boundary condition, the irregular star technique is used in the solution procedure for the Poisson equation of pressure. The distance between the pressure point of each cell and the interface is called the leg-length. The leg-length and the pressure on the interface are used in the Poisson equation instead of the grid spacing and the pressure at the pressure point of the neighboring cell.

In the present computation, the pressure on the interface depends on the fluid flow of the neighboring region. Therefore, the pressure value on the interface is determined by extrapolating the pressure from an adjacent cell to the interface. In fact, the pressure on the

interface is decided by using an equivalent extrapolation in horizontal direction and a linear extrapolation of the acceleration of gravity in a vertical direction. On the interface, velocity extrapolation is also necessary to calculate differential terms near the free surface. When the slope of the interface is greater than 45° , the velocities are horizontally extrapolated from the interested region to the neighboring region, and the velocity gradient in the normal direction is approximately neglected at the interface.

3 Computational results

3.1 Wave generation

In many problems including the free surface, numerical diffusion and damping may have a strong effect on the final result. Hence it is necessary to check the accuracies in properties of numerically generated waves in advance. Figure 1 compares the numerically generated waves at their 10th period with an analytic solution. The height is 0.06m and the wave length is 1.00m. The wave represented by dashed line was computed with the hybrid method. i.e. the marker method is used up to 2m in the x direction and after than the line segment method is combined to treat multi-valued free surface. Significant damping of the wave is present at the third profiles period due to the line segment method. The other wave generated by the marker density method shows a good coincidence to the analytic one.

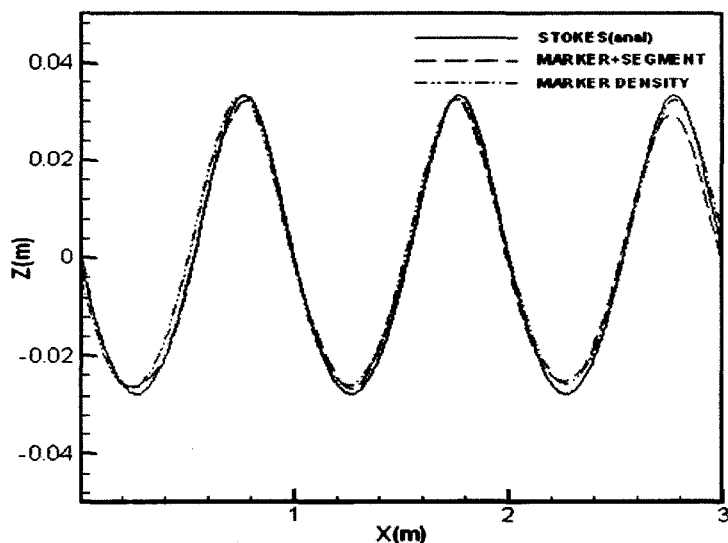


Figure 1: Comparison of Wave($H_0 = 0.06\text{m}$, $T = 1.0$)

3.2 Wave breaking by hybrid method

Breaking waves with various characteristics are simulated by the hybrid method. The wave conditions are shown in Table 1, and the computational domain are shown in Figure 2. Figure 3 and Figure 4 show vorticity contours of a spilling breaker and a plunging breaker. Despite of the different breaker type, similar patterns of motion and vortex

systems are found. It agrees with the postulation by Basco (1985) that both spilling and plunging breakers have similar initial breaking motions, domain but at different scales.

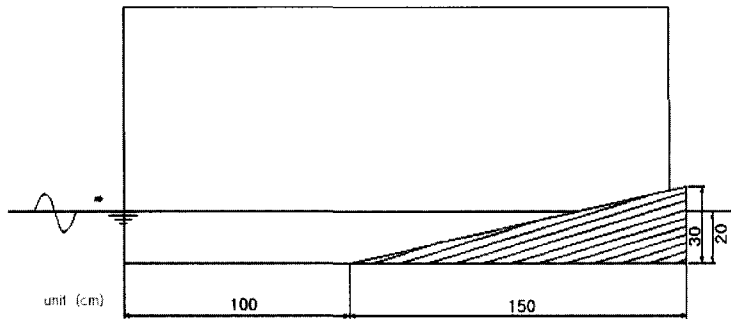


Figure 2: Sketch of the computational

Table 1: Condition of incident waves

CASE	Beach Slope m	Period T(Sec)	Wave Height H ₀ (m)	Wave Length L ₀ (m)	Wave Steepness H ₀ / L ₀	Surf Similarity Parameter ξ _o
1	1/5	0.80	0.040	1.000	0.040	1.000
2		0.80	0.060	1.000	0.060	0.816
3		0.80	0.100	1.000	0.100	0.632
4	1/10	0.80	0.060	1.000	0.060	0.408
5		0.80	0.080	1.000	0.080	0.354
6		1.00	0.066	1.561	0.042	0.488
7		1.13	0.060	2.000	0.030	0.577
8		1.28	0.095	2.570	0.037	0.520
9	1/30	1.75	0.152	4.752	0.032	0.186

All the tested waves are classified in Figure 5 in which they are divided into spilling and plunging breakers. It shows a good coincidence with the transition value of the surf similarity parameter defined as follows(Battjes 1974).

$$\xi_o = m / (H_0/L_0)^{1/2} \tag{6}$$

surging or collapsing if $3.3 < \xi_o$
 plunging if $0.5 < \xi_o < 3.3$
 spilling if $\xi_o < 0.5$

Wave profiles compared with experimental data by Hino et al (1984) are shown in Figure 6 and 7 in case of 2 and 3, respectively. The present results agree well with them except overturning waves are not shown in the experiment. However, it is expected that plunging breakers will usually occur since the wave conditions are in the plunging breaker region according to the surf similarity parameter.

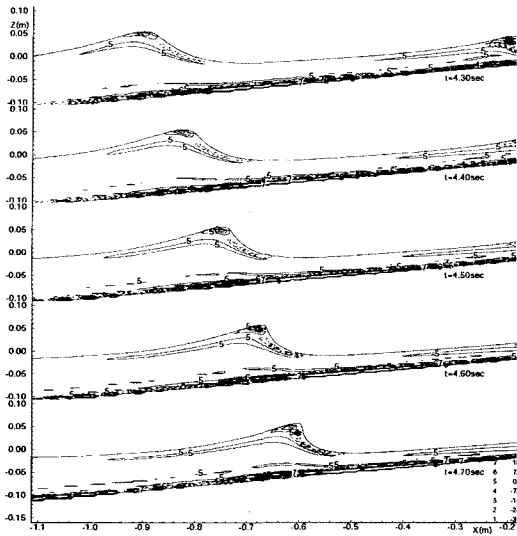


Figure 3: Variation of vorticity contours with an advancing breaker (case 5)

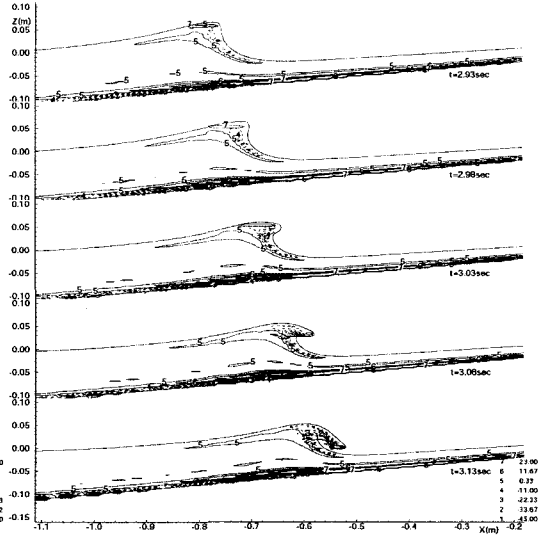


Figure 4: Variation of vorticity contours with an advancing breaker (case 8)

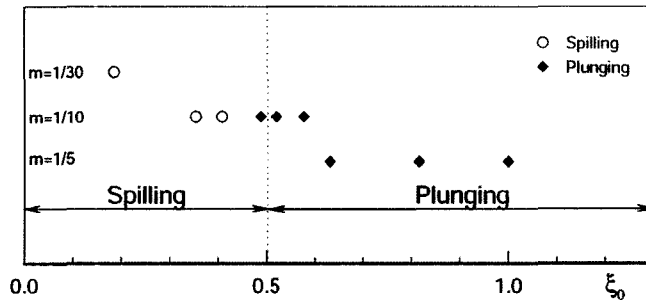


Figure 5: Breaker type classification at each of the present computations

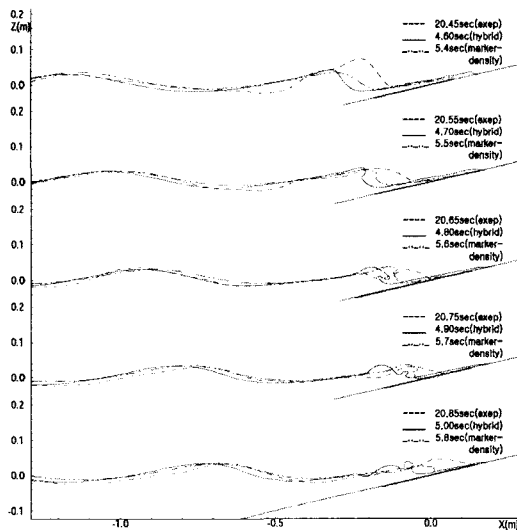


Figure 6: Comparison of free surface profiles (case 2)

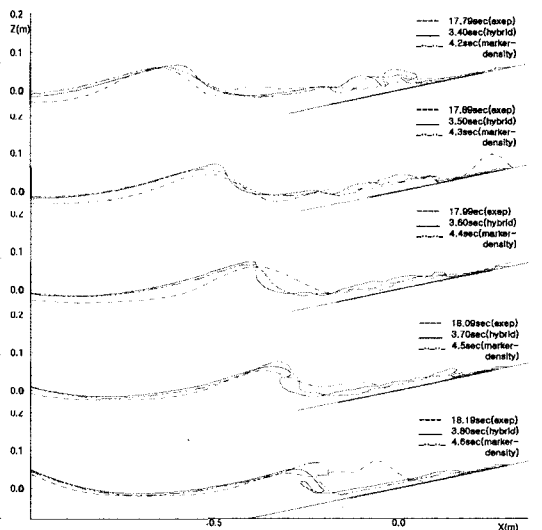


Figure 7: Comparison of free surface profiles (case 3)

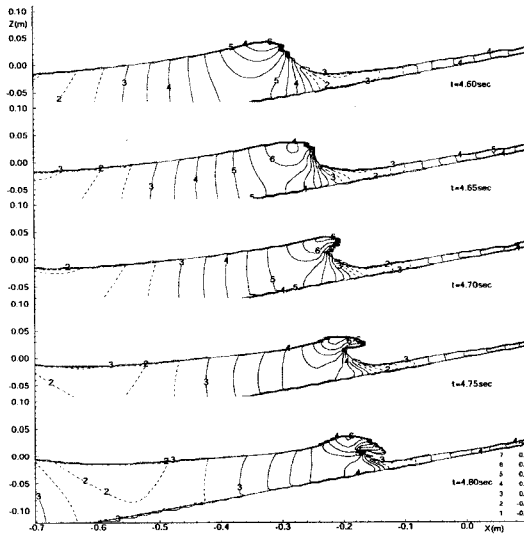


Figure 8: Variation of pressure contours with an advancing breaker (case 2, by [marker+segment] method)

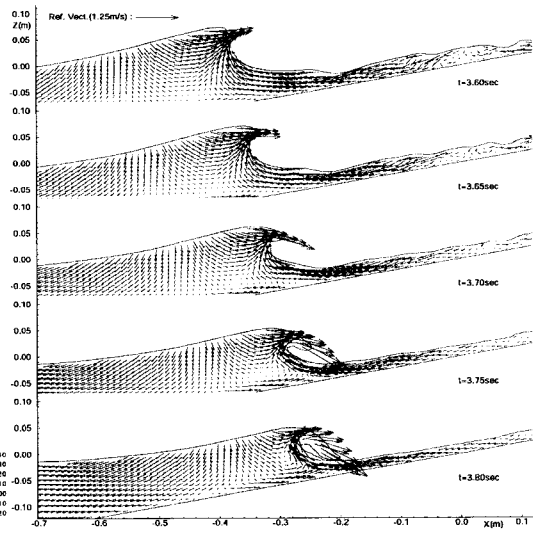


Figure 9: Variation of vectors with an advancing breaker (case 3, by [marker+segment] method)

Pressure contours and velocity vectors are shown in Figure 8 and 9, respectively. The large magnitude of pressure and velocity vector at the wave crests are shown when the waves commence to overturn.

3.3 Wave breaking by marker density method

In spite of its successes, the hybrid method can not yield a credible solution if the plunging jet impinges the undisturbed water. Marker density method is employed to overcome such difficulties for the simulation of wave breaking phenomena. The beach have the two different case of wave steepness for computations, 0.06 and 0.10(case 2 and 3), that is, the wave conditions are the same as in section 3.2.

Figures 6 and 7 computed by the hybrid and the marker density method, respectively, show that the wave profiles from the marker density method show the better coincidence with experimental data than the results of hybrid method. Figure 10 shows the high pressure regions as the wave overturns and impinges. That is same pattern with in section 3.2. Velocity vectors in case of 3 are shown in figure 11, which are also computed with the marker density method. Since the wave amplitude is 5/3 times larger than the preceding case, the possibility for plunging breaker is larger than before. A good-looking plunging breaker occurred almost a period earlier than those for the case 2. The velocity vectors also become larger as the wave overturns.

4 Conclusions

In this paper nonlinear free surface phenomena in the surf zones are numerically simulated by the hybrid method and the marker-density method in the rectangular mesh system. The process of the evolution of plunging breakers is numerically simulated including the second plunging jet. In spite of the approximations in the free surface and the body

boundary, the present method, especially the marker density method gave good results quantitatively as well as qualitatively.

The present computational method can be easily applied to practical engineering problems especially including complicated nonlinear free surface phenomena. For more accurate results, further efforts should be devoted to the consideration of the surface tension, viscous stress and turbulence modeling and to invention of a method which can treat after-breaking phenomena.

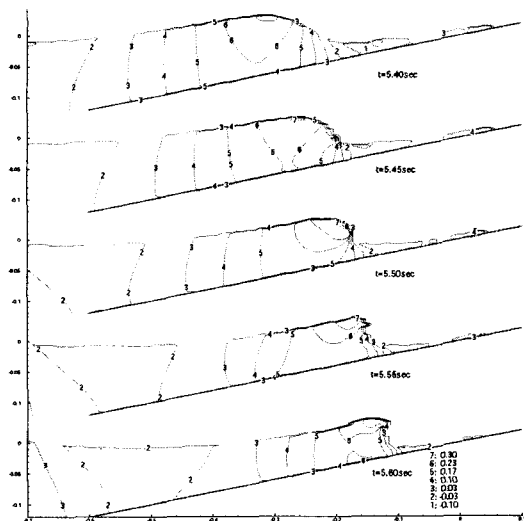


Figure 10: Variation of pressure contours with an advancing breaker (case 2, by marker density method)

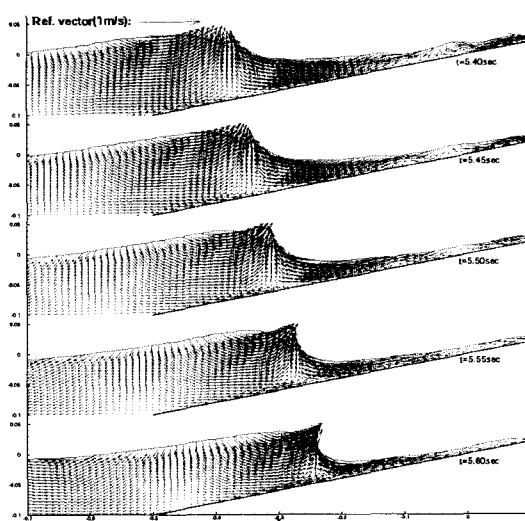


Figure 11: Variation of vectors with an advancing breaker (case 3, by marker density method)

Acknowledgements

This research is partly supported by Inha University and RRC for Transportation System of Yellow Sea.

References

- Basco, D.R. 1985. A qualitative description of wave breaking. *J. Waterway, Port, Coastal, and Ocean Eng.*, **111**, 2, 171-188.
- Battjes, J.A. 1974. Surf similarity. *Proc. of 14th Coastal Eng. Conf.*, ASCE, 460-480.
- Battjes, J. A. 1988, Surf-zone dynamics. *Ann. Rev. Fluid Mech.*, **20**.
- Chan, R.K.C. and R.L. Street. 1970. SUMMAC-A numerical model for water waves. Technical Report, **135**
- Chen, G., C. Kharif, S. Zaleski and J. Li. 1999. Two-dimensional navier-stokes simulation of breaking waves. *Physics of Fluids*, **11**, 1, 121-133.
- Galvin, C.J. 1968. Breaker type classification on three laboratory beaches. *J. Geophys. Res.*, **73**.

- Grilli, S.T. 1993. Modeling of nonlinear wave motion in shallow water. Computational Methods for Free and Moving Boundary Problems in Heat and Fluid Flow, Computational Mechanics Publications.
- Heo, J.K. and Y.G. Lee. 1996. A numerical simulation of two-dimensional nonlinear waves in surf zone. Proc. KOJAM '96, 309-317.
- Hino, T., H. Miyata, H. Kajitani, and M. Kanai. 1984. A numerical solution method for nonlinear shallow water waves (second report). J. Soc. Naval Arch. Japan, **154**, 29-39.
- Hirt, C.W. and B.D. Nichols. 1981. Volume of fluid (VOF) method for the dynamics of free boundaries. J. Computational Physics, **39**, 201-225.
- Hwung, H.H., C. Lin and C.C. Kao. 1988. The Turbulent Flow Fields and Vortex Structures inside Surf Zone, Nonlinear Water Waves, Springer-Verlag, Berlin.
- Koshizuka, S., A. Nobe and Y. Oka. 1998. Numerical analysis of breaking waves using the moving particle semi-implicit method. Int. J. Numer. Mech. Fluids, **26**, 751-769.
- Le Mehaute, B. 1976. An Introduction to Hydrodynamics and Water Waves, Springer-Verlag, Berlin.
- Lin, P. and P.L.F. Liu. 1998. A numerical study of breaking waves in the surf zone. J. Fluid Mech., **359**, 239-264.
- Monaghan, J.J. 1994. Simulating free surface flows with SPH. J. Computational Physics, **110**.
- Peregrine, D.H. 1983. Breaking waves on beaches. Ann. Rev. Fluid Mech., **15**, 149-178.
- Perlin, M. and J. He. 1996. An experimental study of deep water plunging breakers. Phys. Fluids, **8, 9**, 2365-2374.
- Smith, E. R. and N.C. Kraus. 1990. Laboratory study on macro-features of wave breaking over bars and artificial reefs. Technical Report CERC-90-12, U. S. Army Engr. WES, Vicksburg, Mississippi, 307-323.
- Sussman, M., P. Smereka and S. Osher. 1994. A level set approach for computing solutions to incompressible two-phase flows. J. Computational Physics, **114**, 146-159.